PULSE FORM OPTIMIZATION FOR MIMO SONAR SYSTEMS

Sven Schröder German Aerospace Center, Institute for the Protection of Maritime Infrastructures, Germany
Sarah Barnes German Aerospace Center, Institute for the Protection of Maritime Infrastructures, Germany
Dieter Kraus City University of Applied Sciences Bremen, Germany
Anton Kummert University of Wuppertal, Germany

1 INTRODUCTION

Essential for the MIMO principle is the ability to separate the transmitter signals from each other at the receiver-side signal processing. Signal separation methods are typically divided into the categories Time-Division-Multiplexing (TDM), Frequency-Division-Multiplexing (FDM) as well as Code-Division-Multiplexing (CDM) [12]. When applying the TDM method to MIMO sonars, the transmitter signals are emitted in different time slots to be able to separate them in time after receiving. However, this implies a longer overall ping period within the observed scene may change. These changes may impede the coherent processing of the consecutively emitted transmitter signals and can result in a reduced angular resolution enhancement. The FDM method is based on a division of the available frequency band in sub-bands. This reduces the bandwidth of each transmitter signal, which consequently leads to a decreased range resolution. In addition, coherent processing of frequency divided signals causes artefacts in the Point-Spread-Function (PSF) of the system [13, 3]. This paper is focussed on the CDM method which uses coding techniques to enable a simultaneous transmission of all transmitter signals in the same frequency band. The receiver-side pulse separation and compression are realized with a bank of matched-filters.

This paper deals with the optimisation of MIMO pulse sets with respect to the sidelobes in the distance domain of the PSF of the system. In the literature, pulse optimisation is usually applied to single transmitter signals, trying to minimise the sidelobe level in the autocorrelation [6]. This ignores the coherent signal processing of MIMO systems, where constructive interference can lead to high sidelobes in the PSF. However, integrating the computationally complex simulation environment into the optimisation slows it down significantly, which is why a simplified form with sufficient predictive power of sidelobes in the PSF is to be found. In this work, three cost functions are compared with each other and used to optimise an Orthogonal-Frequency-Division-Multiplexing (OFDM) signal set. In Section 2 the used OFDM signal is described in more detail. Section 3 describes the cost function and optimisation of the transmitter signal set. The results of the optimisation are presented in Section 4. Finally, Section 4 summarises the work.

2 TRANSMITTER SIGNAL

One in the MIMO radar literature often considered transmitter signal candidate is the OFDM signal, cf. [9, 10, 8]. OFDM signals have their origin in communications technology and represent a comparatively new field of research for application in MIMO sonar systems. The principle is based on a multiplexing technique using orthogonal carrier frequencies. For this purpose, the transmitter frequency band is divided into sub frequency bands B_{sub} whose width depends on the length of the OFDM signal by the orthogonality condition

$$T = \frac{1}{B_{\mathrm{sub}}}. \tag{1}$$

If this condition is satisfied, the carrier frequencies lie in the first null of the sinc function of the adjacent carrier frequencies in the frequency domain. In the time domain, each carrier sine wave has an integer number of periods, which leads to a zero crossing at the start and end of each carrier. A single OFDM signal is defined by

$$s_{\mathrm{OFDM}}(t) = \sum_{m=0}^{N_c-1} c_m \cdot e^{j2\pi f_m t}, \;\; t \in [0, T] \tag{2}$$

with

$$f_m = f_0 + mB_{\mathrm{sub}} \quad \text{and} \quad N_c = BT, \tag{3}$$

and the sequence

$$c_m \in \{-1, 1, -j, j\}; \quad \text{for} \quad m = 0, ..., N_c - 1, \tag{4}$$

whereby each carrier frequency contains two bits of information.

3 SIGNAL SET OPTIMISATION

For the optimisation of a mathematical problem, its quality must be translated into a scalar value using a cost function, which can be minimised by varying the input parameters. In this case, it must be determined which properties of a MIMO transmitter signal set are decisive for the performance of the entire system and how these can be quantified. In the literature, the approach of using properties from auto- and cross-correlations for pulse optimisation is often chosen (cf. [2, 12, 11, 1, 17]). One method is to minimise the Generalised-Integrated-Sidelobe-Level (GISL), which is defined as

$$\mathrm{GISL}^{(p)}_{\Omega_{\mathrm{ML}},\Omega_{\mathrm{SL}}}(AC) = \left(\frac{\int_{\Omega_{\mathrm{SL}}} |AC(\tau)|^p d\tau}{\int_{\Omega_{\mathrm{ML}}} |AC(\tau)|^p d\tau} \right)^{2/p}, \tag{5}$$

where p is an arbitrarily selectable integer hyperparameter, Ω_{ML} is the range of the mainlobe and Ω_{SL} is that of the sidelobes (cf. [14, 4, 5, 7]). If $p = 2$ is selected, Equation (5) corresponds to the Integrated-Sidelobe-Level (ISL). For $p \longrightarrow \infty$, Equation (5) converges to the infinity norm $|\cdot|^2_\infty$ and corresponds to the Peak-to-Sidelobe Level Ratio (PSRL), which is a metric frequently used in radar pulseform design in addition to the ISL [6].

In the literature the described metric is commonly used for the optimisation of autocorrelation functions of individual transmitter signals. However, for the use of multiple transmitter signals in a MIMO-CDM system, the characteristics of all transmitter signals and their interaction are crucial. The properties of the PSF, which describes the resolution behaviour and the characteristics of sidelobes in the angle-distance domain, would therefore be decisive for the consideration of the overall system. This is because the PSF includes all effects that can be caused by the coherent superposition of several transmitter signals. Figure 1 shows an example of the PSF of a MIMO system using OFDM pulses. The effects of the

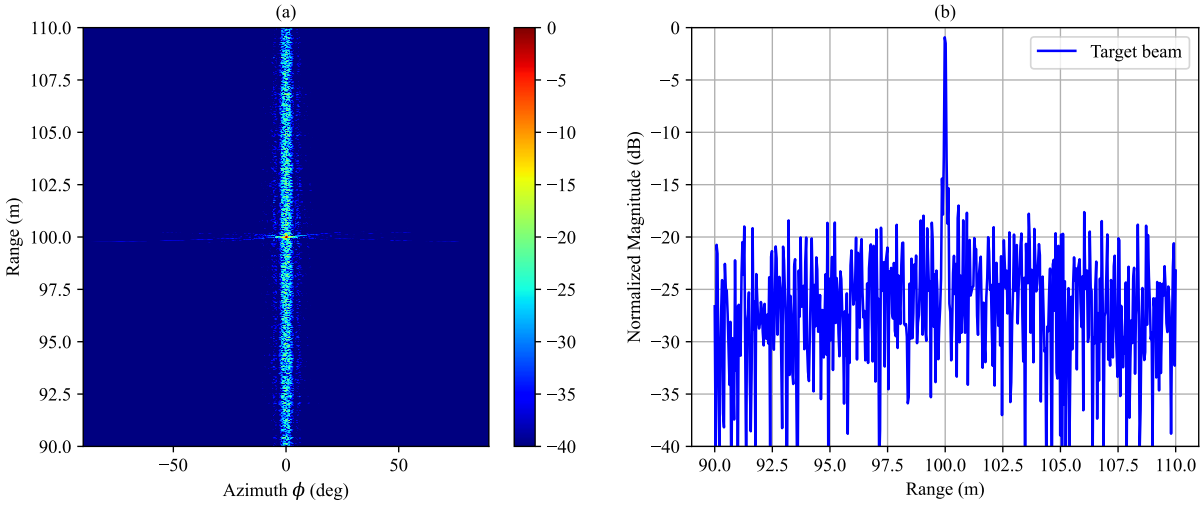

Figure 1: (a) PSF ***of a MIMO system with*** $N = 32$ ***receivers and*** $M = 4$ ***transmitters using OFDM transmitter signals; (b) Target beam signal*** $s_{\mathrm{TB}}(r)$ ***at*** $\phi = 0\,°$ ***which contains major parts of the cross-correlation noise***

sidelobes in the auto- and cross-correlation are most evident in a small area around the target beam signal $s_{\mathrm{TB}}(r) = \mathrm{PSF}(0, r)$, where r is the range. To simplify the optimisation of the PSF, it should be therefore sufficient to consider the target beam signal for the cost function. Applying the GISL on $s_{\mathrm{TB}}(r)$ as a metric leads to the cost function

$$f_1(\mathbf{x}) = \mathrm{GISL}^{(p)}_{\Omega_{\mathrm{ML}},\Omega_{\mathrm{SL}}}(s_{\mathrm{TB}}, \mathbf{x}), \tag{6}$$

where $\mathbf{x}$ is a vector which contains all pulse parameters. The area of the mainlobe Ω_{ML} is defined by

$$\Omega_{\mathrm{ML}} = [R - \frac{c}{2B}, R + \frac{c}{2B}], \tag{7}$$

with the sound velocity c, the target distance R and the signal bandwidth B. The area of the sidelobes is defined by

$$\Omega_{\mathrm{SL}} = [R - cT, R + cT] \setminus \Omega_{\mathrm{ML}}, \tag{8}$$

with the pulse length T.

To evaluate the target beam signal the sonar system has to be modelled and simulated. The simulation environment has been developed in earlier work (cf. [15, 16]) which provides reliable results, as acoustic paths and sonar signal processing are modelled precisely. However, the evaluation is computationally intensive and therefore unsuitable for optimisations with a large number of evaluations of the cost function. A reduction in computational effort of the cost function is therefore required, from which the result of the Equation (6) can be reliably inferred. Extending the optimization of the autocorrelation that is often proposed in the literature, an evident approach would be to analyse the auto- and cross-correlations of the M individual pulses separately and to combine the results incoherently to a scalar value. For this, the GISL of all auto- and cross-correlations of a MIMO pulse set is determined. Overall, this cost function results in

$$f_2(\mathbf{x}) = \frac{1}{M^2}\left(\sum_{m=0}^{M-1} \mathrm{GISL}^{(p)}(AC_{\mathbf{x},m,m}) + 2\sum_{m=0}^{M-2}\sum_{m'=m+1}^{M-1} \mathrm{GICL}^{(p)}(CC_{\mathbf{x},m,m'})\right), \tag{9}$$

where for the evaluation of the cross-correlations the Generalised-Integrated-Cross-correlation-Level

$$\mathrm{GICL}^{(p)}(CC) = \left(\frac{\int_{-T}^{T} |CC(\tau)|^p d\tau}{\mathrm{IML}_{AC}} \right)^{2/p}, \tag{10}$$

is used with the Integrated-Mainlobe-Level (IML) of all autocorrelations

$$\mathrm{IML}_{AC} = \frac{1}{M} \sum_{m=0}^{M-1} \left(\int_{\Omega_{\mathrm{ML}}} |AC_{\mathbf{x},m,m}(\tau)|^p d\tau \right) \tag{11}$$

as the mainlobe reference level. With this approach, the correlation functions of the transmitter signal set are thus evaluated individually, whereby the cost function value is composed of the sum of the partial evaluations. This method is an obvious extension of the optimisation of autocorrelation functions presented in the literature in order to evaluate a set of pulses. However, the phases of the individual correlation functions are not considered. It can be assumed that due to the coherent MIMO processing, constructive interference of the correlation functions can lead to sidelobes in the PSF, which do not occur in the individual correlation functions.

In order to include the effect of MIMO signal processing, all correlation functions of the pulse set are first coherently summed before the GISL is determined. This corresponds to an approximation of the target beam signal at the position of a single scatterer in the far field and is defined as

$$f_3(\mathbf{x}) = \mathrm{GISL}^{(p)} \left(\sum_{m=0}^{M-1} \sum_{m'=0}^{M-1} C_{\mathbf{x},m,m'} \right) \tag{12}$$

To test both simplified cost functions, a set of randomly selected pulse parameters $(\mathbf{x}_0, ..., \mathbf{x}_{K-1})$ is evaluated with the presented cost functions f_1, f_2 and f_3 with the parameter $p = 2$, where f_1 is considered as ground truth, since it is based on a comprehensive simulation of the entire MIMO system. Thereby the OFDM signal has a pulse length of $T = 20\,\mathrm{ms}$ and a Bandwidth of $B = 20\,\mathrm{kHz}$, which results in the total number of carrier $N_c = 400$. Figure 2 shows in (a) the cost function values for $K = 1000$ runs, where the $k = 1, ..., K$ trials were resorted according to increasing function values of f_1, as well as in (b) the resulting target beam signal for the worst ($k = K$) and the best ($k = 1$) evaluation.The function values of f_3 follow those of f_1 sufficiently to be able to draw mutual conclusions about the optimum set of parameters $\mathbf{x}$. The cost function f_2, on the other hand, provides completely independent values and does not allow a joint conclusion to be drawn about an optimal pulse set. This shows that optimising a cost function that incoherently superimposes the auto- and cross-correlation does not necessarily lead to low sidelobes in the target beam signal, and therefore in the PSF. The assumptions made in Equation (12) lead to a highly simplified and efficient, but sufficiently accurate cost function and should therefore be used for optimisation in this work. Equation (6) should be used for the final assessment of the results.

Up to this point, the parameter space of the entire pulse set $\mathbf{s} = (s_0, s_1, ..., s_{M-1})$ was specified with $\mathbf{x}$, but not described in more detail. The properties of the parameter space are essentially dependent on the pulseform or the mapping between the pulse parameter and the parameter space designed for the optimisation algorithm. The differentional evolution optimisation algorithm used in this work is suitable for finding a global minimum in a continuous space $\mathbb{R}^{\kappa}$. However, an OFDM symbol is coded using the bit sequence $\mathbf{c}$ with the length $N_{\mathrm{bit}} = 2BT = 2N_c$. To represent the bit sequence in a continuous parameter space, it is divided into 32 bit blocks, which are represented by an floating point number $x_k \in [0, 1]$. The structure of the parameter vector $\mathbf{x}$ results from the concatenation of all pulse parameters, as shown in Figure 3.

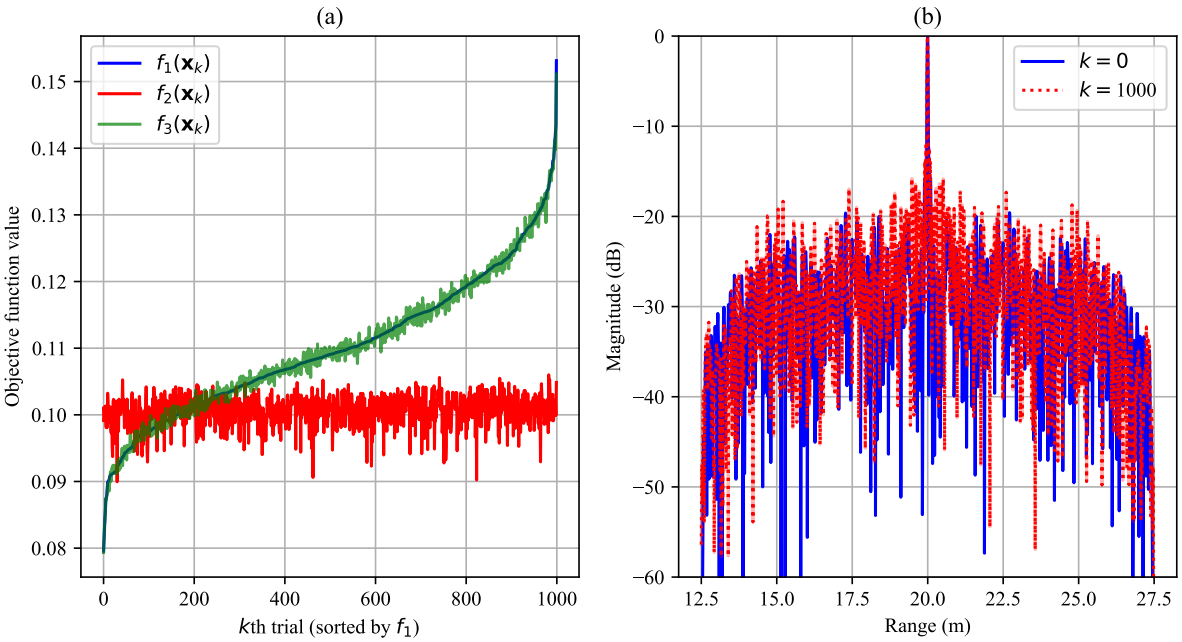

Figure 2: Comparison of the different cost functions

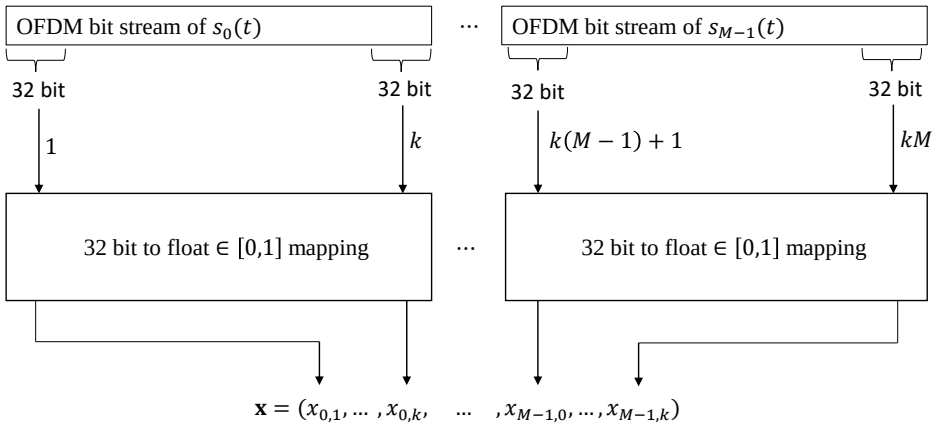

Figure 3: Principle of the parameter space mapping

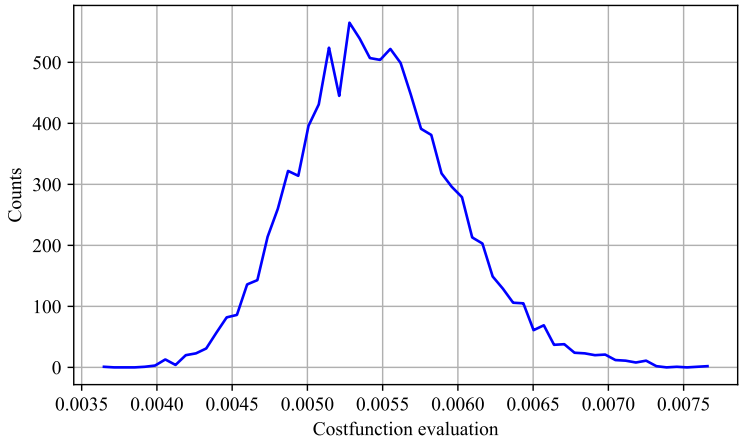

Figure 4: Histogram of cost function evaluations of randomly generated transmitter signal sets

A metric is required to assess the success of an optimisation, as the global minimum is unknown. The evaluation $f_3(\mathbf{x})$ of the cost function of $K = 10000$ randomly selected parameter vectors $\mathbf{x}$ is used as a statistical comparison variable. The distribution of $f_3(\mathbf{x})$ is shown in Figure 4. The aim of optimisation is to improve the results compared to a random search.

4 RESULTS

Figure 5 shows in (a) the evaluations of the cost function $f_3(\mathbf{x})$ for the random search sorted by function value (blue), the best candidates for the initialisation of the optimization (dashed red) and in (b) the results of the iteration steps of the optimisation (green). In this study, the optimisation was limited to $N_i = 1000$ iteration steps. In the first 200 iterations, the optimisation was able to achieve significant improvements compared to randomly selected pulse parameters. Figure 6 shows an example of the target beam signal to be optimised for a randomly selected parameter vector in (a) and the optimised parameter vector $\mathbf{x}_{\mathrm{opt}}$ in (b). The sidelobes are visibly reduced in the optimised case. This is also reflected in the entire PSF, as shown in Figure 7. The PSFs shown are normalised and show values above the threshold value $\Gamma = -30\,\mathrm{dB}$. By comparing the area above the threshold value of both PSFs with

$$\epsilon_\Gamma = \frac{\int_\phi \int_r 1_{[\Gamma,\infty)}(\mathrm{PSF}_{\mathrm{opt}}(\phi,r))}{\int_\phi \int_r 1_{[\Gamma,\infty)}(\mathrm{PSF}_{\mathrm{rand}}(\phi,r))}, \quad 1_A(x) = \begin{cases} 1 & x \in A \\ 0 & \text{else} \end{cases}, \tag{13}$$

this results in $\epsilon_{-30\,\mathrm{dB}} = 0.8929$ for the example shown in Figure 7. The characteristics of sidelobes are also lower in the optimised PSF than in the randomly selected signal set.

Also when comparing the GISL between the median of the randomly generated and the optimized pulse sets with

$$\xi = \frac{\mathrm{median}\,(f_{\mathrm{rand}})}{f_{\mathrm{opt}}} \tag{14}$$

shows an improvement of $\xi = 1,65$.

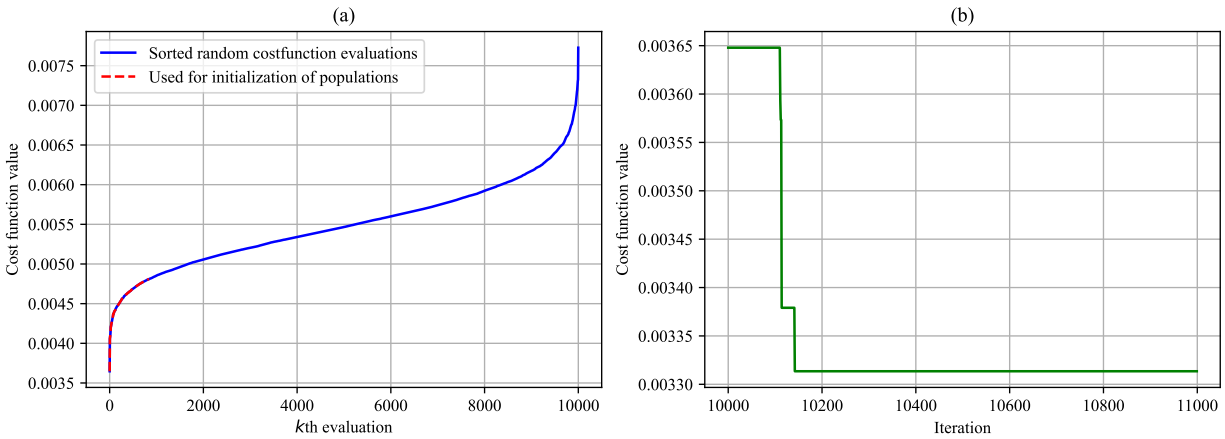

Figure 5: (a) Cost function values of the randomly generated OFDM transmitter signal sets (sorted); (b) Cost function values for each iteration step of the optimisation

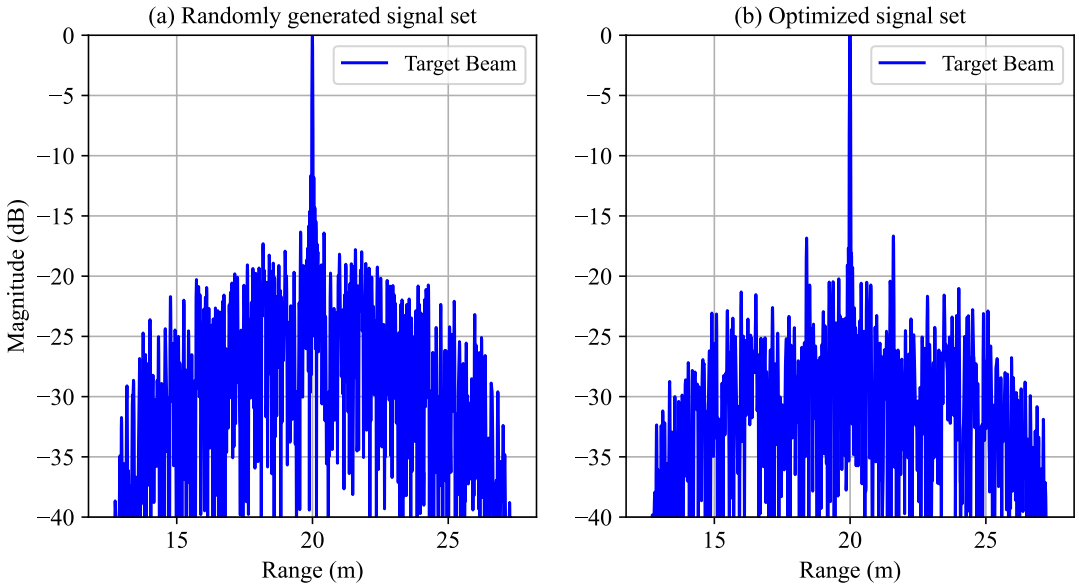

Figure 6: $\mathrm{PSF}(0, r)$ ***for a randomly generated and an optimised OFDM transmitter signal set***

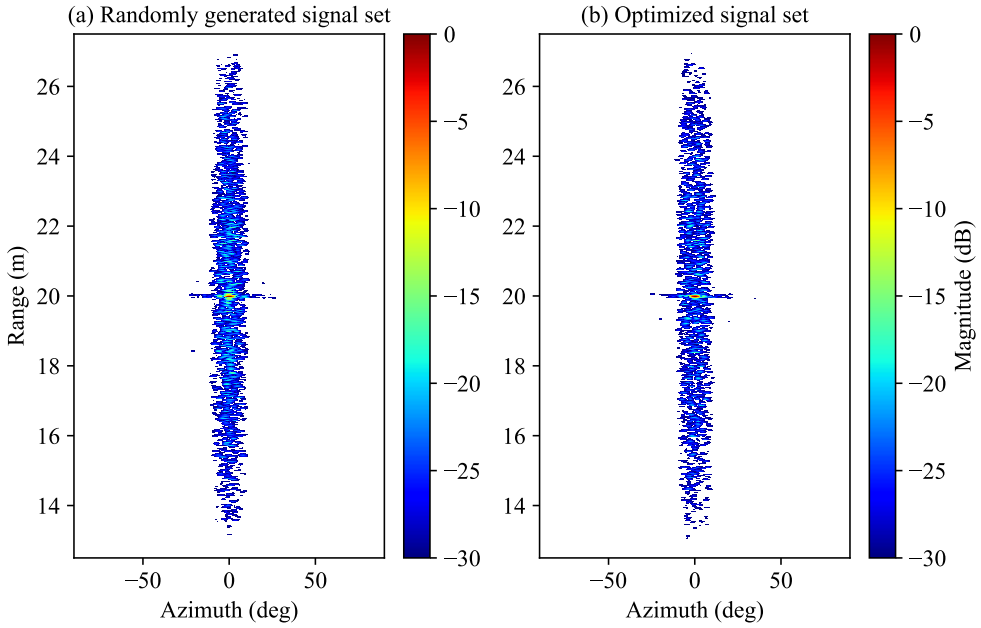

Figure 7: $\mathrm{PSF}(\phi, r)$ ***for a randomly generated and an optimised OFDM transmitter signal set***

5 SUMMARY

In this work, the optimisation of MIMO transmitter signal sets with regard to the sidelobe level in the point spread function was investigated. Various cost functions based on the correlation functions of the transmitter signals and a complex simulation of the entire sonar system were compared with each other. It was found that the separate consideration and optimisation of individual auto- and cross-correlations does not necessarily lead to good results in the PSF. The integrated sidelobe level in the coherent superposition of all transmitter signals proves to be a sufficient compromise between computational effort and the predictive power of sidelobes in the PSF. The found cost function is used to optimise a set of four OFDM signals. The results show a significant suppression of the sidelobes in the PSF. If the area with levels above the threshold value of -30 dB between a randomly selected pulse set and the optimised pulse set is considered, this is reduced by over 10% as a result of the optimisation. This improvement leads to less background clutter in the application of a sonar system and to the avoidance of ambiguities in the sonar image.

REFERENCES

[1] Ting Bai, Nae Zheng, and Song Chen. “OFDM MIMO radar waveform design for targets identification”. In: *ETRI Journal* 40.5 (2018), pp. 592–603. DOI: 10.4218/etrij.2018-0010.

[2] Shannon Blunt et al. “Polyphase-coded FM (PCFM) radar waveforms, part II: optimization”. In: *IEEE Transactions on Aerospace and Electronic Systems* 50.3 (2014), pp. 2230–2241. DOI: 10.1109/TAES.2014.130362.

[3] David Cohen, Deborah Cohen, and Yonina C. Eldar. “High Resolution FDMA MIMO Radar”. In: *IEEE Transactions on Aerospace and Electronic Systems* 56.4 (2020), pp. 2806–2822. DOI: 10.1109/TAES.2019.2958193.

[4] Michael S. Davis and Aaron D. Lanterman. “Minimum integrated sidelobe ratio filters for MIMO radar”. In: *IEEE Transactions on Aerospace and Electronic Systems* 51.1 (2015), pp. 405–416.

[5] Hamid Esmaeili Najafabadi, Mohammad Ataei, and Mohamad Farzan Sabahi. “Chebyshev chaotic polynomials for MIMO radar waveform generation”. In: *IET Radar, Sonar & Navigation* 11.2 (2017), pp. 330–340. DOI: 10.1049/iet-rsn.2016.0270.

[6] David G. Felton and David A. Hague. “Gradient-Descent Based Optimization of Multi-Tone Sinusoidal Frequency Modulated Waveforms”. In: *OCEANS 2023 - Limerick*. Piscataway, NJ: IEEE, 2023, pp. 1–7. DOI: 10.1109/OCEANSLimerick52467.2023.10244644.

[7] David A. Hague. “Adaptive Transmit Waveform Design Using Multitone Sinusoidal Frequency Modulation”. In: *IEEE Transactions on Aerospace and Electronic Systems* 57.2 (2021), pp. 1274–1287. DOI: 10.1109/TAES.2020.3046086.

[8] Gor Hakobyan. *Orthogonal frequency division multiplexing multiple-input multiple-output automotive radar with novel signal processing algorithms*. 2018. DOI: 10.18419/opus-9830.

[9] Hui Li et al. “Orthogonal frequency division multiplexing linear frequency modulation signal design with optimised pulse compression property of spatial synthesised signals”. In: *IET Radar, Sonar & Navigation* 10.7 (2016), pp. 1319–1326. DOI: 10.1049/iet-rsn.2015.0642.

[10] MengJiao Li, Wen-Qin Wang, and Zhi Zheng. “Communication–embedded OFDM chirp waveform for delay–Doppler radar”. In: *IET Radar, Sonar & Navigation* 12.3 (2018), pp. 353–360. DOI: 10.1049/iet-rsn.2017.0369.

[11] Melissa Marchand et al. “Multi-input multi-output waveform optimization for synthetic aperture sonar”. In: *Detection and Sensing of Mines, Explosive Objects, and Obscured Targets XXI*. Ed. by Steven S. Bishop and Jason C. Isaacs. SPIE Proceedings. SPIE, 2016, p. 98231X. DOI: 10.1117/12.2229054.

[12] Yan Pailhas and Yvan Petillot. “Wideband CDMA Waveforms for Large MIMO Sonar Systems”. In: *2015 Sensor Signal Processing for Defence (SSPD)*. 2015, pp. 1–4.

[13] Olivier Rabaste et al. “Signal waveforms and range/angle coupling in coherent colocated MIMO radar”. In: *2013 International Conference on Radar (Radar 2013)*. Piscataway, NJ: IEEE, 2013, pp. 157–162. DOI: 10.1109/RADAR.2013.6651977.

[14] William Roberts et al. “Probing Waveform Synthesis and Receiver Filter Design”. In: *IEEE Signal Processing Magazine* 27.4 (2010), pp. 99–112. DOI: 10.1109/MSP.2010.936724.

[15] Sven Schröder et al. “Experimental investigation of a virtual planar array for MIMO sonar systems”. In: *International Conference on Underwater Acoustics*. Proceedings of Meetings on Acoustics. ASA, 2022, p. 070005. DOI: 10.1121/2.0001591.

[16] Sven Schröder et al. “Study on pulse form design for monostatic MIMO sonar systems”. In: *OCEANS 2023 - Limerick*. Piscataway, NJ: IEEE, 2023, pp. 1–8. DOI: 10.1109/OCEANSLimerick52467.2023.10244369.

[17] Yujiu Zhao et al. “OFDM wavefroms designed with piecewise nonlinear frequency modulation pulse for MIMO radar”. In: *International Journal of Remote Sensing* 39.23 (2018), pp. 8746–8765. DOI: 10.1080/01431161.2018.1490978.